Development of a 3-Stage ADR for Space including CCA 50 mK Characterization

D. A. Paixao Brasiliano[1], J-M. Duval[1], N. Luchier[2], S. D'Escrivan[3], J. André[3]

[1]Univ. Grenoble Alpes, INAC-SBT, F-38000 Grenoble, France
[2]CEA, INAC-SBT, F-38000 Grenoble, France
[3]CNES, 18, Avenue Edouard Belin, 31401 Toulouse Cedex 9, France

ABSTRACT

Highly sensitive detectors required for astrophysics missions, such as ATHENA and SPICA, require temperatures as low as 50mK to operates with the targeted sensitivity. Adiabatic demagnetization refrigerator (ADR) systems are a suitable solution for sub-kelvin space applications. We present a design of a 3 stage ADR for the range 4 K – 50 mK with 0.45 μW of cooling power at 50 mK. Results of our preliminary study and design of the main components such as the heat switches and paramagnetic materials are discussed. We also report a sub kelvin characterization of the magneto caloric properties of chromic caesium alum (CCA) and compare its performance as a magnetic refrigerant to chromic potassium alum (CPA).

INTRODUCTION

The next generation of astronomy missions requires cooling down to 50 mK for highly sensitive detectors such as used in SPICA/SAFARI[1] for far IR observations and ATHENA/X-IFU[2] for X-ray spectroscopy. ADRs are a suitable solution for sub kelvin space applications for a broad range of starting temperature[3]. For instance, the last stage of the cryogenic chain of the SXS instrument on Astro-H uses a three stage ADR, combined with an intermediary 1.2 K liquid helium cryostat or a 4.5 K in degraded mode, to produce 50 mK for cooling down the X-ray detector array[4].

We hereby report our study of a one-shot multi-stage ADR for the 4 K – 50 mK temperature range having 0.45 μW of cooling power at 50 mK for an autonomy of 24 hours. Our pre-study indicated that a system composed of three stages represents a good compromise between the overall mass and the system complexity. We present the design that was chosen and its leading criteria. We also report on the impact of using CCA as an alternative magnetic refrigerant for CPA for the low temperature stage.

DESIGN

The design of our three-stage ADR is shown in Figure 1. Each stage is composed of a solid state refrigerant (a paramagnetic material), a superconducting magnet and a gas-gap heat switch (HS). Similar to the design proposed by Shirron et. al.[5], the stages are set in series, which allows the multi-stage ADR to cover the large range of temperature that is required. For convenience, the stages are called S1, S2 and S3, from the high temperature stage to the low temperature; and HS1,

Cryocoolers 19, edited by S.D. Miller and R.G. Ross, Jr.

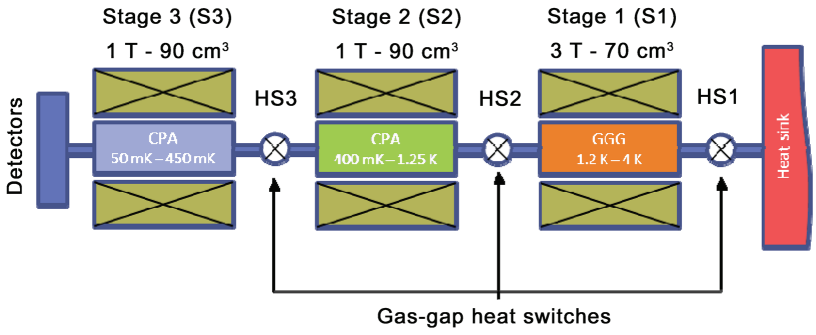

Figure 1. Schematic of the three-stage ADR. The magnetic fields indicated are averaged over the salt pill volume.

HS2 and HS3, their respective heat-switches. Some of the main elements that drive the design, namely the magnetic refrigerants and heat-switches, are discussed.

The paramagnetic materials chosen for this initial design are GGG and CPA for the high and low temperature stages, respectively. These materials are typical used for their respective temperature range and are readily available at the required amounts. In parallel, work has been done to identify, grow and characterize more efficient materials that can replace GGG and CPA in future designs, and will reduce the overall system mass.

The role of the heat switches is to provide a high thermal conductance in the closed or ON position, for magnetizing the stages and to otherwise isolate them in the open or OFF position. A high ON conductance shortens the recycling time and/or decreases the temperature gradient through the HS, and increases the heat-transfer efficiency. A low OFF conductance reduces the parasitic heat load on each stage.

^{3}He gas gap heat-switches are suitable for all stages. The coldest temperature at which the HS3 needs to be ON is 400 mK. At this temperature, care must be taken to prevent the formation of liquid by limiting the amount of helium inside the switch. Condensation of liquid would deteriorate the operation and the switching time. The HS design adopted is similar to the heat-switches developed for the Herschel space telescope program[6] in order to benefit from its heritage.

The choice of the number of stages is a trade-off between the overall complexity of the system, which increases with the number of stages, and the total mass. The former is related to the management of a higher number of elements and their associated electronics. The latter can be reduced by increasing the number of stages through reduction in the parasitic heat load and the magnetic field requirements[5]. Considering the one-shot operation, the use of classical magnetic refrigerants such as GGG and CPA and the chosen thermal budget, the gain from 3 to 4 stages is marginal in terms of mass. The conclusion reached was that a 3 stages system represents a good compromise for the design.

The primary criterion for sizing the stages is that each one must withstand 24 h at its low operating temperature under nominal heat load conditions, the starting point being its high operating temperature and maximum magnetic field as shown in Figure 1. The second criterion is that the upper stage must be able to recharge the lower stage in one cycle in order to minimize the recycling time.

In principle, only the extreme operating temperatures of the system are fixed (4 K and 50 mK). The intermediate temperatures are chosen in order to minimize the global mass. This choice depends mainly on the magnetic refrigerant properties and on the HS OFF conductance. Combined, those two factors imply that the highest stage temperature ratios rT (i.e. ratio between higher and lower stage temperatures) are found for the coldest stages in order to minimize the required magnetic field and parasitic heat load. Figure 1 shows that rT is close to 3.3 for S1, 3.1 for S2 and 9 for S3. The estimated parasitic heat load through the heat-switches are 20.9 μW for HS1, 1.1 μW for HS2 and about 70 nW for HS3.

The total heat losses of each stage during the "cold phase" is composed of the parasitic losses due to the heat switch, Kevlar suspensions and attached to the heat sink at 4 K, the latter being neg-

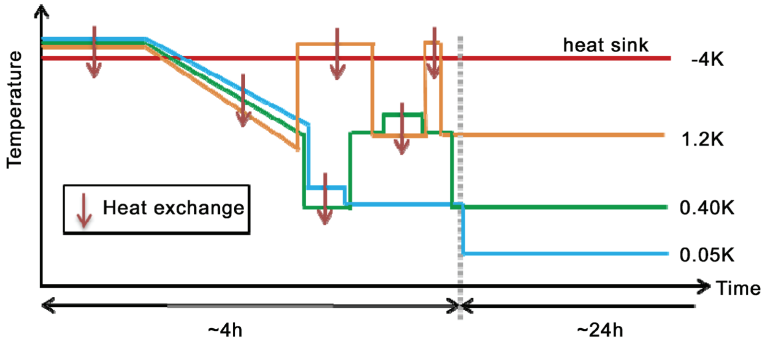

Figure 2. Schematic of the warm start recycling strategy

ligible. In order to reduce the heat load of S2 and S3, S1 is used to intercept heat from the Kevlar suspensions of S2 and S3, as well as S2 is used to intercept heat from S3. In this configuration, heat losses due to the Kevlar suspensions are estimated to be 18 µW for S1, 1.9 µW for S2 and 0.05 µW for S3, respectively. The net cooling power available at 1.2 K, 400 mK and 50 mK are estimated to be 15 µW, 1.2 µW and 0.45 µW, respectively. The power of S1 and S3 are typical external heat loads for the 1.2 K and 50 mK temperatures (e.g. precooling of wires reaching S3 and sensors load). The cooling power of S2 is a consequence of the recycling strategy we have chosen (i.e. S2 must be able to recharge S3 in one cycle) and may be used as well for precooling the sensor wires.

RECYCLING STRATEGIES

Two recycling strategies that will be employed in function of the starting condition of the multi-stage ADR is reported in this section. For this, two extreme conditions are considered: warm and cold start. The former is characterized by all stages being at the sink temperature. The latter is characterized by all stages being at their nominal cold temperature and correspond to the end of the previous cycle. At the beginning of both conditions, the stages are fully discharged i.e. in zero magnetic field.

The warm start procedure is represented in Figure 2. The cycle starts with the 3 ADR stages recharging their magnetic field and rejecting the heat load to the sink at 4 K. The second step takes advantage of the great cooling capacity of S1 at high temperatures for precooling the other stages: with HS1 OFF and HS2 and HS3 ON, S1 is slowly demagnetized in order to efficiently cool S2 and S3 down to about 1 K. This procedure allows the reduction of the recycling time compared with the alternative of independently demagnetizing the 3 stages for a few reasons: the heat exchanges for recycling stages 2 and 3 happen at high temperature, where the thermal conductance of the heat switches is enhanced. For the same magnetic field, the entropy variation at high temperature is significantly smaller than at low temperature; after the precooling, S2 is already fully recharged and can then carry on the final step to recharge of S3. The third step completes the recycling procedure: S3 is recharged by S2 at 400 mK while S1 is recharged at 4 K. Once finished, S2 is recharged by S1 at 1.2 K and then S1 is recharged at 4 K. Now that all stages are fully charged, they are demagnetized to attain their nominal temperatures. A proportional–integral–derivative (PID) algorithm is used to maintaining them for about 24 h under nominal heat load.

The cold start procedure is represented in Figure 3. The stages are first magnetized to their nominal hot temperature, which allows S1 to be recharged and the reduction of heat losses over S2 and S3. After being recharged, S1 recharges S2, which can then recharge S3. S1 afterwards recharges S2 and is finally recharged at 4 K. After demagnetization, the 3 stages are ready to deliver their cold temperature for about 24 h under nominal heat load.

CHARACTERIZATION OF CCA

The viability of using CCA for space ADR was first reported by Hagmann et al[7]. CCA has the same chemical composition of CPA with potassium replaced by caesium. Furthermore, they have

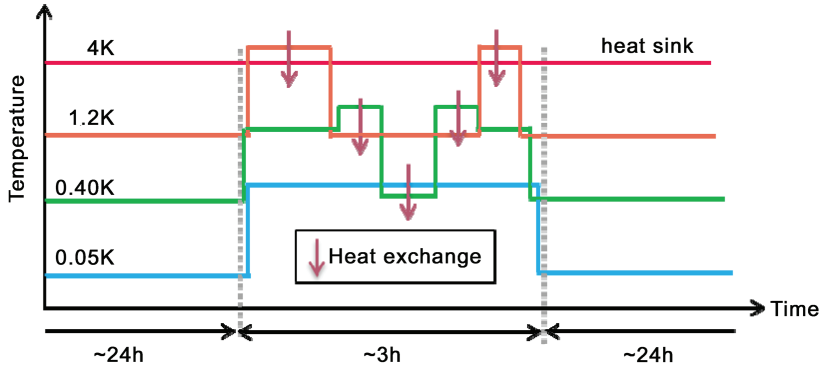

Figure 3. Schematic of the cold start recycling strategy

the same magnetic ion and many close properties such as effective angular momentum J, Landé factor g and molar volume of magnetic ions. It has been reported that CCA has greater resistance to thermal degradation than CPA, withstanding temperatures up to 50 °C in a sealed pill with no observable degradation, while the CPA was found to be degraded in the same conditions[7]. The degradation temperature is an important concern if the satellite is baked out.

CPA has been characterized during the characterization of an ESA engineering model of a hybrid 50 mK ADR/sorption cooler previously developed in our laboratory[8]. The CPA stage operates in the 450 mK – 50 mK range and is fully magnetized at 0.8 T using a heat sink at about 300 mK. CCA has been chosen to be characterize in similar conditions and using the same hybrid cooler.

The CPA pill was replaced by a CCA pill containing 102 g of the salt (0.178 mol) grown onto copper wires as has been described by Timbie et al[9]. The pill filling rate is close to 82% according to the density reported by Hagmann et al[7] and may be improved with further development of the growth process. The impact of the relatively low filling rate may affect the thermal resistance of the bus but it's unlikely to significantly affect the magnetocaloric properties of the salt.

The CCA pill was equipped with a 50 mK Lakeshore Ruthenium Oxide thermometer and a heater.

Specific Capacity, Thermal Gradient and Parasitic Heat Load Measurement Methods

Figure 4 summarizes how the specific heat, thermal gradient and parasitic heat load are measured: the evolution of the pill temperature is measured before, during and after a heat pulse is applied to the pill.

When the pill is heated, a thermal gradient appears between the extremity of the thermal bus where the thermometer is mounted and the salt. It is assumed that the salt temperature is homogeneous and that the majority of the pill heat capacity is composed by the salt. The total gradient, which includes the gradient in the copper bus and at the interfaces, can then be measured from $\Delta T_{decoupling}$ and the applied power (see Figure 4a).

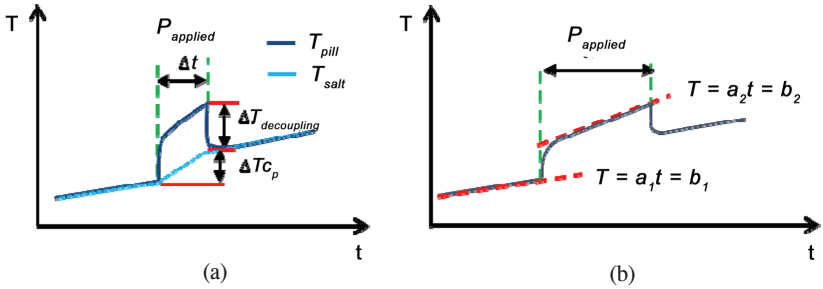

Figure 4. Method of measurement of specific heat, thermal conductance (left) and parasitic heat load (right).

Measurements of the pill thermal gradient showed that it could be predicted by the power law $\Delta T_{decoupling} = 3926 \cdot PT^{1.92}$, with the applied power P in µW and the mean temperature T of the salt pill in mK. The thermal decoupling of the CCA pill is 2.1 mK/µW at 50 mK as compared to 1.1 mK/µW for the CPA salt pill[8].

Specific capacity can be measured from the applied power and its duration. If the parasitic heat load can be neglected compared to the applied power, the amount of energy transferred to the pill is PΔt. Thus, the pill heat capacity is given by C(T, B) = PΔt/ΔT, where B is the magnetic field applied by the superconducting coil. If the parasite heat load is not negligible, P must be replaced by P + Pparasitic.

The parasitic heat load can be estimated by comparing the temperature slopes in the presence and absence of a constant applied power. If the temperature variation is small enough, the pill specific heat can be considered constant and the parasitic heat load can be calculated as function of the applied power and the ratio $r = a_1 / a_2$ (see Figure 4b) as follow: Pparasitic = Papplied*r/(1-r). To maximize the sensitivity of these measurements, the applied power is chosen to be of the same order of magnitude as the estimated heat load.

A parasitic heat load of 0.12 µW at 50 mK has been measured, which is in agreement with the calculated load from parasitic conductivity.

Specific Heat

The power and duration used in this measurement ranges from 2 µW to 50 µW with a duration from 5 min to 20 min depending on the temperature and magnetic field. The parasitic heat load is limited to 5% of the applied power in the worst case scenario.

As verified by Luchier et al[8] for a similar pill design, the components of the pill other than CCA have a negligible contribution to the pill specific capacity in the temperature range covered by our measurements. Thus, the specific heat of CCA is given by $C_{CCA} = P\Delta t/\Delta T/n$, where n = 0.178 mol of CCA.

The results are shown in Figure 5, as well as our measurements of CPA specific heat done in similar experimental conditions. The similar behavior of both pills suggests that the magnetocaloric properties are close. Therefore, it is expected that CCA could replace CPA in an ADR stage without a major change in performance.

Available Energy

In these measurements, the salt is magnetized at the 300 mK heat sink and then is thermally isolated by turning the HS OFF. At this point, a power is applied by the heater and the salt is demagnetized. The demagnetization is controlled by a PID algorithm so the pill temperature is kept constant until the magnetic field is depleted. The available energy at a temperature T is given by the integral over time of the total load reaching the pill. With no power applied, the pill was able to reach 28 mK when completely demagnetized from 325 mK and 0.8 T.

A measurement done at 56 mK with Papplied = 1.57 µW is shown in Figure 6. The measured parasitic heat load is less than 10% of the applied power. The temperature of the salt is estimated to be 52 mK due to the pill thermal decoupling. For the measurements at 100 mK and 200 mK, the parasitic heat load is less than 5% of the applied power.

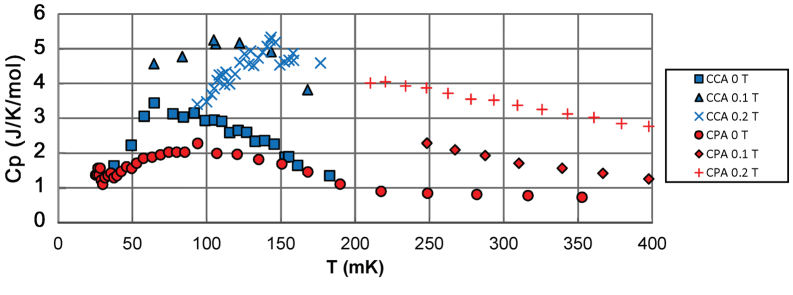

Figure 5. Specific heat measurements of CCA and CPA in different magnetic fields.

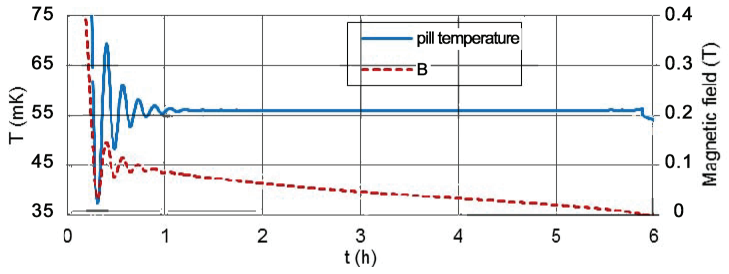

Figure 6. Temperature regulation of CCA salt pill at 56 mK with 1.57 ∝W applied load

Table 1. Available energy in function of the working temperature. The predicted energy was calculated using the theoretical entropy diagram published by Hagmman et al[7].

T0 (mK)	B0 (T)	T (mK)	P (μW)	Autonomy (h)	Predicted energy (J/mol)
315	0.8	52	1.7	5.6	0.19
302	0.8	100	5.4	6	0.65
305	0.8	200	10.6	6	1.28

Table 1 summarizes the results of these measurements. The starting magnetic field is 0.8 T for all cases but the starting temperatures are slightly different, varying between 302 mK and 315 mK. Direct and precise comparison of available energy is limited by experimental uncertainties in these types of measurements, such as the thermometers precision at high and low temperatures, magnetic field homogeneity over the salt pill volume and temperature gradient through the thermal bus. The estimation of each contribution is difficult but we think it can explain the variations of Table 1. Nevertheless, we validated that CCA can be considered a replacement of CPA for producing 50 mK from temperatures up to about 400 mK without major impact on the stage design considering our experimental precision.

CONCLUSION

A one-shot 3 stage ADR for space working on the 4 K – 50 mK temperature range with 24 h autonomy with 0.45 μW at 50 mK has been designed. The prototype is currently in its final stage of fabrication and will be characterized this fall.

The CCA in the 50 mK – 400 mK temperature range has also characterized using a maximum magnetic field of 0.8 T. This material gives the possibility of a higher temperature bake-out. This first characterization shows that the CCA has similar magneto-caloric properties to CPA within the precision of experimental measurement. Further characterization will be needed for precisely quantifying the differences between both salts and for extending the temperature and magnetic field ranges.

CURRENT DEVELOPMENTS

In parallel to this work, alternative materials with better predicted performances are currently being developed such as YbGG ($Yb_3Ga_5O_{12}$). The difficulty for their availability in the short term and large quantities prevents us from implementation in this prototype. This work will be presented in a future publication.

ACKNOWLEDGMENT

This work is financially supported by CNES and CEA. We wish to thank Lionel Dubois and Johann Breitenstein from CEA/SYMMES for their work on the development of CCA growth process. Thanks also to Jean-Louis Durand for the experimental work and his expertise in the design and set up. Thanks to Florian Bancel for the design of the complete model.

REFERENCES

1. Duband, L., Duval, J.M., Luchier, N., D'Escrivan, S., "SPICA/SAFARI sub-Kelvin cryogenic chain," *Cryogenics*, Vol. 52, Issues 4-6 (April-June 2012), pp. 145-151.
2. Ravera, L., et al. "The X-ray integral field unit (X-IFU) for Athena," *Proc. SPIE 9144 Space Telescopes and Instrumentation* 2014: Ultraviolet to Gamma Ray, 91442L (July 24, 2014)
3. Shirron, P. J., Canavan, E.R., DiPirro, M.J., Tuttle, J.G., Yeager, C.J., "A multi-stage continuous-duty adiabatic demagnetization refrigerator," *Adv. in Cryogenic Engineering*, Vol. 45B, Springer US, pp. 1629-1638.
4. Shirron, P.J., Kimball, M.O., Wegel, D.C., Canavan, E.R., DiPirro, M.J., "Design of a 3-stage ADR for the soft x-ray spectrometer instrument on the ASTRO-H mission," *Proc. SPIE 7732,* Space Telescopes and Instrumentation 2010: Ultraviolet to Gamma Ray, 773212 (July 29, 2010)
5. Shirron, P.J. "Applications of the magnetocaloric effect in single-stage, multi-stage and continuous adiabatic demagnetization refrigerators,"*Cryogenics, Vol.* 62 (July-August 2014), pp. 130-139.
6. Duband, L. "A thermal switch for use at liquid helium temperature in space-borne cryogenic systems," *Cryocoolers 8*, Springer US, pp. 731-741.
7. Hagmann, C., Benford, D. J., Richards, P. L., "Paramagnetic salt pill design for magnetic refrigerators used in space applications," *Cryogenics,* Vol. 34, Issue 3 (March 1994), pp. 213-219.
8. Luchier, N., Duval, J.M., Duband, L., Tirolien, T., "Performances of the 50mK ADR/sorption cooler," *Cryogenics,* Vol. 52 Issues 4 -6 (April-June 2012), pp. 152-157.
9. Timbie, P.T., Bernstein, G.M., Richards, P.L., "Development of an adiabatic demagnetization refrigerator for SIRTF," *Cryogenics,* Vol. 30 Issue 3 (March 1990), pp. 271-275.